Khuri-Treiman Representation and Perturbation Theory

JOHN B. BRONZAN*
Palmer Physical Laboratory, Princeton University, Princeton, New Jersey
AND
CLAUDE KACSER†
Columbia University, New York, New York
(Received 8 July 1963)

It is characteristic of decay amplitudes that the spectral functions for their integral representations have branch points overlapping the integration contour. For the amplitude satisfying the Khuri–Treiman dispersion representation, the prescription for passing the branch points is shown to be incomplete. The full prescription is obtained using perturbation theory as a guide. It turns out that the perturbation theory prescription contradicts the "naive" dispersion theory prescription in part, even in the physical decay region of the amplitude. An interpretation is offered for this contradiction. In the perturbation analysis it is found that a non-Landau or second-type singularity appears on the unphysical boundary of the physical sheet of the decay amplitude. In view of this unexpected result, the usual Landau analysis of perturbation amplitudes is extended to include examination of the singularity of the complex non-Landau surface on the physical sheet. Such an extension is valuable when an explicit formula for the spectral function is unavailable. Here the extended Landau analysis facilitates comparison of the present results with previous work on decay amplitudes. One part of the discussion presents and makes use of an analysis in which an internal mass is taken as a complex variable.

1. INTRODUCTION

DECAY amplitudes to three-body final states depend on two scalar variables. In general such amplitudes have complex branch points when considered as an analytic function of one of the variables, with the second variable fixed in its physical range.[1] This circumstance has forced physicists to concentrate on the subset of decay amplitudes in perturbation theory which have only normal branch points. In particular, Khuri and Treiman[2] have presented a dispersion representation for the sum of this subset of amplitudes. Although we are not concerned here with the question of the accuracy of the Khuri and Treiman (KT) amplitude as an approximation to the true decay amplitude, we point out that the KT amplitude includes the effect of two-body rescattering of the final-state particles upon leaving the decay region. This property has led to interest in the KT representation as a model for production processes where final-state scattering is important.[3] Of course the representation has been applied to the discussion of decay processes as well.[2]

Up to the present time, calculations based on the KT representation have started with one of three simplifying restrictions. Either the final-state scattering has been assumed to be weak, or only one pair of final-state particles has been permitted to rescatter strongly, or one of the final-state particles has been assumed to be infinitely massive. In essence these restrictions have been made because the dynamical equation which follows from the KT representation is a singular linear integral equation whose kernel has branch points which overlap the contour of integration. Since the kernel must be defined in part by analytic continuation, the proper manner of passing the branch points becomes a matter requiring a careful discussion. The restrictions mentioned above allow one to avoid the problem of the branch points, either by removing the difficult addend of the kernel altogether, or by greatly simplifying the analytic structure of the kernel.

It is the purpose of this paper to obtain a well-defined dynamical equation from the KT representation. With this equation one can study the influence of overlapping final-state rescattering on decay and production amplitudes without any dynamical or kinematical restrictions. We follow Peierls and Tarski[3] in designating final-state rescattering to be overlapping when one or more of the final-state particles scatters strongly with the other two. In the course of our analysis we encounter several results which are interesting outside the context of the KT representation. In particular, we find that a non-Landau singularity can appear on the unphysical boundary of the physical sheet of the triangle diagram in perturbation theory. We therefore extend the usual Landau analysis to include the possibility of singularities on the complex non-Landau surface. We also compare our results with a previous treatment of decay amplitudes in perturbation theory,[4] elucidating a subtle point involving the choice of complex variables.

In Sec. 2 we write down the KT representation and its attendant dynamical equation. We consider the analytic continuation of the kernel of the equation, and show that the continuation involves us in an ambiguity.

* National Science Foundation predoctoral fellow. Work supported in part by the U.S.A.F. Office of Scientific Research. Present address: Department of Physics, Massachusetts Institute of Technology, Cambridge, Massachusetts.
† Work supported in part by the U. S. Atomic Energy Commission.

[1] See, for example, G. Barton and C. Kacser, Nuovo Cimento **21**, 988 (1961).
[2] N. N. Khuri and S. B. Treiman, Phys. Rev. **119**, 1115 (1960).
[3] R. F. Peierls and J. Tarski, Phys. Rev. **129**, 981 (1963). This paper contains a useful bibliography.
[4] G. Barton and C. Kacser, Nuovo Cimento **21**, 593 (1961).

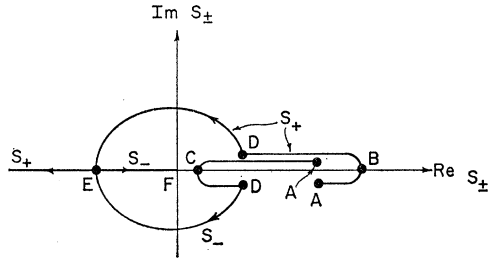

FIG. 1. Paths of the branch points $s_\pm(\lambda^2)$ (cf. 2.7).

In Sec. 3 we circumvent the ambiguity by studying the analytic properties of one of the perturbation amplitudes contributing to the KT sum. We find that the kernel given by perturbation theory is different from the kernel given by KT even in part of the physical region. This finding is discussed and related to the choice of complex variables mentioned above. In Sec. 4 the problems of choice of complex variables and non-Landau or second-type singularities are studied from a more general point of view; in particular we present a perturbation theory analysis of the singularities of the triangle graph, as a function of an internal mass variable. The techniques are general, and should prove useful in many problems.

2. THE KHURI-TREIMAN DYNAMICAL EQUATION

For simplicity consider the decay of a spin zero particle of mass $M>3$ into three identical spin zero particles, a, b, and c, each of mass 1. Again for simplicity, we ignore isotopic spin and assume that only s-wave scattering between any pair of the outgoing particles is large. We denote the two-particle scattering amplitude in the center-of-mass system by $g=e^{i\delta}\sin\delta$. Our process depends upon two of the three scalar variables s_a, s_b, s_c.

$$\begin{aligned} s_a&=(p_M-p_a)^2,\\ s_b&=(p_M-p_b)^2,\\ s_c&=(p_M-p_c)^2,\\ p_M{}^2&=M^2,\quad p_a{}^2=p_b{}^2=p_c{}^2=1. \end{aligned} \tag{2.1}$$

These variables are related by the relation

$$s_a+s_b+s_c=M^2+3. \tag{2.2}$$

Let the decay amplitude for particle M be $M(s_a,s_b,s_c)$. The KT dispersion representation for M is[5]

$$\begin{aligned} M(s_a,s_b,s_c)=&\frac{1}{\pi}\int_4^\infty \frac{d\lambda^2 g^*(\lambda^2)M_0(\lambda^2)}{\lambda^2-s_a-i\epsilon}\\ &+\frac{1}{\pi}\int_4^\infty \frac{d\lambda^2 g^*(\lambda^2)M_0(\lambda^2)}{\lambda^2-s_b-i\epsilon}\\ &+\frac{1}{\pi}\int_4^\infty \frac{d\lambda^2 g^*(\lambda^2)M_0(\lambda^2)}{\lambda^2-s_c-i\epsilon}. \end{aligned} \tag{2.3}$$

[5] Of course, one should perform at least one subtraction. We do not exhibit this explicitly since it does not affect the results.

Here $M_0(s_a)$ is the s-wave projection of M in the frame $\mathbf{p}_b+\mathbf{p}_c=\mathbf{p}_M-\mathbf{p}_a=0$.

$$\begin{aligned} M_0(s_a)&=\frac{1}{2}\int_{-1}^{1} d(\cos\theta_{bc})M(s_a,\cos\theta_{bc}),\\ \cos\theta_{bc}&=R(s_a,s_b)/[U(s_a)]^{1/2},\\ R(s_a,s_b)&=-s_a{}^2+(M^2+3-2s_b)s_a,\\ U(s_a)&=s_a[s_a-4][s_a-(M-1)^2][s_a-(M+1)^2]. \end{aligned} \tag{2.4}$$

We specify $[U(s_a)]^{1/2}>0$ for s_a within the physical decay limits $4\leqslant s_a\leqslant(M-1)^2$.

We obtain the KT dynamical equation for $M_0(s_a)$ by integrating (2.3) over $\cos\theta_{bc}$.

$$\begin{aligned} M_0(s_a)=&\frac{1}{\pi}\int_4^\infty \frac{d\lambda^2 g^*(\lambda^2)M_0(\lambda^2)}{\lambda^2-s_a-i\epsilon}\\ &+\frac{2}{\pi}\int_4^\infty d\lambda^2 K(s_a,\lambda^2-i\epsilon)g^*(\lambda^2)M_0(\lambda^2), \end{aligned} \tag{2.5}$$

where

$$\begin{aligned} K(s,\lambda^2-i\epsilon)&=\frac{s}{[U(s)]^{1/2}}\int_{-1}^{1}\frac{dx}{x-R(s,\lambda^2-i\epsilon)/[U(s)]^{1/2}}\\ &=\frac{s}{[U(s)]^{1/2}}\ln\frac{R(s,\lambda^2-i\epsilon)-[U(s)]^{1/2}}{R(s,\lambda^2-i\epsilon)+[U(s)]^{1/2}}. \end{aligned} \tag{2.6}$$

Clearly, once we have $M_0(s)$ on the arc $4\leqslant s<\infty$, we can recover the KT amplitude from (2.3). We note that the boundary prescription $\lambda^2\to\lambda^2-i\epsilon$ for $K(s,\lambda^2)$ is uniquely dictated to us by the arguments presented in the KT paper.

In order that (2.5) be completely defined, we must specify $K(s,\lambda^2-i\epsilon)$ throughout the quadrant $4\leqslant s$, $\lambda^2<\infty$. However, in our angular integration we are forced to take $4\leqslant s\leqslant(M-1)^2$, so K must be defined in part by continuing s above $(M-1)^2$. This in turn requires us to study the analytic structure of K, considered as a function of s, near the arc $4\leqslant s<\infty$. λ^2 is to be taken as a parameter along the arc $4\leqslant\lambda^2<\infty$.

We see from (2.6) that $K(s,\lambda^2-i\epsilon)$ has logarithmic branch points whenever $R(s,\lambda^2-i\epsilon)/[U(s)]^{1/2}=\pm1$. This equation may be solved for s, and for fixed λ^2 the two branch points in the s plane are located at

$$\begin{aligned} s&=s_\pm(\lambda^2)-i\epsilon[\partial s_\pm(\lambda^2)/\partial\lambda^2],\\ s_\pm(\lambda^2)&=\{R(\lambda^2,0)\pm[U(\lambda^2)]^{1/2}\}/2\lambda^2. \end{aligned} \tag{2.7}$$

As λ^2 moves along its arc, the branch points move along the trajectories shown in Fig. 1. The displacement of the branch points from the real s axis, due to ϵ, is shown only when $\mathrm{Re}\,s>4$. As λ^2 increases from 4 to ∞, the branch points pass through the letters on the trajectories in alphabetical order. Values of s and λ^2 associated with the letters are given in Table I.

One problem is immediately evident from Fig. 1. As we increase s above $(M-1)^2$, we cross the trajectory of $s_+(\lambda^2)$ at B. Let us postpone dealing with this point until Sec. 3. Then we see that there are no logarithmic branch points above $s=(M-1)^2$ when λ^2 is on the relevant arc. However, there are two additional possible branch points of K to consider. These are the branch points of $[U(s)]^{1/2}$ at $s=(M-1)^2$ and $s=(M+1)^2$. There is a cut between these two branch points, and since $[U(s)]^{1/2}>0$ for $4\leqslant s\leqslant(M-1)^2$, we see that just below the cut $[U(s)]^{1/2}=+i|U(s)|^{1/2}$, while just above the cut $[U(s)]^{1/2}=-i|U(s)|^{1/2}$.

From the integral representation of $K(s,\lambda^2-i\epsilon)$, (2.6), we see that for s just below $(M-1)^2$ the pole of the integrand is near infinity, and we are on the principal (real) branch of the logarithm. Thus, just above $(M-1)^2$,

$$K(s,\lambda^2-i\epsilon)=[2s/\mp|U(s)|^{1/2}]\times\tan^{-1}[\pm|U(s)|^{1/2}/R(s,\lambda^2)]. \quad (2.8)$$

The upper sign goes with the upper branch of $[U(s)]^{1/2}$, and the lower sign goes with the lower branch. Since we start out on the principal (vanishing) branch of the arctangent at $(M-1)^2$, K is independent of the branch of $[U(s)]^{1/2}$ chosen, and has no cut between $(M-1)^2$ and $(M+1)^2$, even though $[U(s)]^{1/2}$ does.

For $M+1<\lambda^2$, $R(s,\lambda^2)$ does not vanish between $s=(M-1)^2$ and $s=(M+1)^2$. The arctangent remains on its principal branch and returns to zero at $s=(M+1)^2$. Thus for $M+1<\lambda^2$, K is analytic at $s=(M+1)^2$, and there is no problem in continuing K. On the other hand, if $4\leqslant\lambda^2<M+1$, $R(s,\lambda^2)$ changes from positive to negative as s moves from $(M-1)^2$ to $(M+1)^2$. Then $s=(M+1)^2$ becomes a branch point of K. We point out that this is a second-type or non-Landau singularity,[6] and that it arises because the arctangent has moved onto its second sheet.

We summarize by saying that $K(s,\lambda^2-i\epsilon)$ has a branch point at $s=(M+1)^2$ for $4\leqslant\lambda^2<M+1$. Since $U(s)$ is independent of λ^2, the presence of the small imaginary term does not move the non-Landau singularity off the real s line. We must look beyond the KT representation to determine how to pass the branch point, and we do this by turning to perturbation theory. We note here that perturbation theory will turn out to disagree with the KT specification of the branch of K. We will find that in perturbation theory $K(s,\lambda^2-i\epsilon)$ is always analytic at $s=(M+1)^2$.

TABLE I. Values of s and λ^2 when the branch points of $K(s,\lambda^2-i\epsilon)$ are located at the lettered points in Fig. 1.

Point	λ^2	s
A	4	$\frac{1}{2}(M^2-1)$
B	$M+1$	$(M-1)^2$
C	$\frac{1}{2}(M^2-1)$	4
D	$(M-1)^2$	$M+1$
E	$(M+1)^2$	$-M+1$
F	∞	0

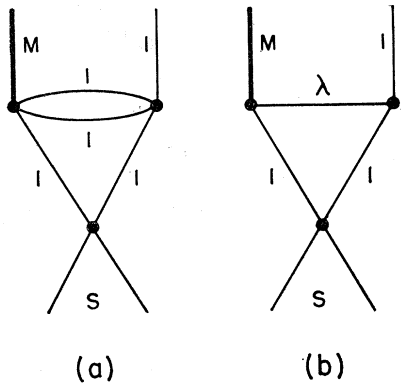

FIG. 2. The relevant perturbation theory diagrams.

3. PERTURBATION THEORY

The diagram we study is shown in Fig. 2(a). The perturbation amplitude corresponding to this diagram is presumably an addend of the KT amplitude. Since the perturbation amplitude represents the situation in which rescattering between one pair of final-state particles is followed by rescattering between a second pair, we are not surprised to find that the spectral function of the dispersion representation for the amplitude involves an integral over K, as in (2.6). Thus we obtain the proper branch of K directly from a study of Fig. 2(a).

Figure 2(a) has already been studied by Barton and Kacser.[4] They show that the amplitude for Fig. 2(a), $F(s,M^2)$, can be expressed as an integral over the amplitude for the simpler triangle diagram of Fig. 2(b). If we call the amplitude for the latter diagram $f(s,M^2,\lambda^2)$,

$$F(s,M^2)=\int_4^\infty d\lambda^2\sigma(\lambda^2)f(s,M^2,\lambda^2), \quad (3.1)$$

where $\sigma(\lambda^2)$ is the renormalized propagator spectral function for the final state particles. Barton and Kacser[4] show that $f(s,M^2,\lambda^2)$ satisfies a normal dispersion representation, and it thus follows that we have a dispersion representation for F.

$$F(s,M^2)=\int_4^\infty \frac{ds'P(s',M^2)}{s'-s-i\epsilon}. \quad (3.2)$$

The spectral function obtained by Barton and Kacser[4] is

$$P(s,M^2)=[(s-4)/s]^{1/2}\int_4^\infty d\lambda^2\sigma(\lambda^2)K(s,\lambda^2). \quad (3.3)$$

Barton and Kacser[4] find that the overlapping branch

[6] See D. B. Fairlie, P. V. Landshoff, J. Nuttall, and J. C. Polkinghorne, J. Math. Phys. 3, 594 (1962), and Phys. Letters 3, 55 (1962). Also see M. Fowler, J. Math. Phys. 3, 936 (1962), and Nuovo Cimento 27, 952 (1963).

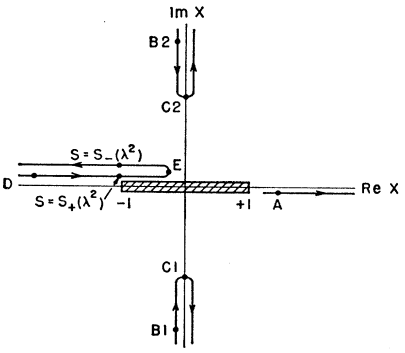

FIG. 3. The path of the pole in the integral representation for K (cf. 2.6).

points of $K(s,\lambda^2)$ are to be removed from the real s axis in (3.3) either by giving M^2 a small positive imaginary part, or by giving λ^2 a small negative imaginary part. They assert that the prescriptions are interchangeable. We find, contrary to this, that it takes some work to show that the two prescriptions yield the same expression for F. As we shall see, it is precisely the appearance of λ^2 rather than M^2 as the second complex variable in (2.6) which leads to the difficulty in the determination of the proper branch of K. In what follows we will first choose λ^2 as a complex variable, and at the end we will show what changes when M^2 is chosen instead.

In the next section we will see that $f(s,M^2,\lambda^2)$ is real for $s<2$ and $\lambda^2>(M-1)^2$. It follows that $K(s,\lambda^2-i\epsilon)$ must be real for all $s\geqslant 4$, and $\lambda^2>(M-1)^2$. This is our reference region for studying K in perturbation theory. To extend this region, we note that Fig. 2(b) represents a definite amplitude for all real $\lambda^2>0$. Thus the proper way to continue K out of the reference region is to obtain K for all s before changing λ^2. Moreover, we note from Fig. 1 that no branch point of K lies above $s=(M+1)^2$. By continuity, for $s>(M+1)^2$, K must be real. Thus our program is to take K to be real, $s>(M+1)^2$. For fixed λ^2 we reduce s towards 4 and take what comes. After we have found K for $s\geqslant 4$ in this way, we reduce λ^2 until some difficulty is encountered. The lettered points of Fig. 1 turn out to divide the real λ^2 line into intervals along which K has uniform analytic properties. We already know that K is real for $\lambda^2>(M-1)^2$. We have three further ranges of λ^2 to consider.

Range 1: $\frac{1}{2}(M^2-1)<\lambda^2<(M-1)^2$

We use the integral representation (2.6) to study K. The motion of the pole of the integrand in the complex x-plane as s is changed is shown in Fig. 3. Starting at A, the pole moves to ∞ along the positive x axis as s approaches $(M+1)^2$. Thus K is real for $s>(M+1)^2$, as required. Just below $s=(M+1)^2$, the pole appears at $B1$ if we take the upper branch of $[U(s)]^{1/2}$, and at $B2$ if we take the lower branch. However, K is independent of which choice we make, for by a trivial change of variables,

$$K(s,\lambda^2-i\epsilon)$$
$$=s/[U(s)]^{1/2}\int_{-1}^{1}\frac{dx}{x-R(s,\lambda^2-i\epsilon)/[U(s)]^{1/2}}$$
$$=-s/[U(s)]^{1/2}\int_{-1}^{1}\frac{dx}{x+R(s,\lambda^2-i\epsilon)/[U(s)]^{1/2}}. \quad (3.4)$$

Thus our earlier result is verified. $K(s,\lambda^2-i\epsilon)$ has no cut between $s=(M-1)^2$ and $s=(M+1)^2$. K is also real between $(M-1)^2$ and $(M+1)^2$

$$K(s,\lambda^2-i\epsilon)$$
$$=-\frac{sR(s,\lambda^2-i\epsilon)}{|U(s)|}\int_{-1}^{1}\frac{dx}{x^2+R^2(s,\lambda^2-i\epsilon)/|U(s)|}$$
$$-\frac{is}{|U(s)|^{1/2}}\int_{-1}^{1}\frac{xdx}{x^2+R^2(s,\lambda^2-i\epsilon)/|U(s)|}. \quad (3.5)$$

The second integrand is odd in x, and vanishes. Finally, it is important that $R(s,\lambda^2)$ does not vanish for $\frac{1}{2}(M^2-1)<\lambda^2<(M-1)^2$. This means that the pole never pushes through the integration contour in Fig. 3. At $C1$ or $C2$, depending on the branch of $[U(s)]^{1/2}$, the pole reverses its motion and withdraws to ∞ as s approaches $(M-1)^2$. Just below $(M-1)^2$, the pole appears at D on the negative x axis, and it reaches $x=-1$ when $s=s_+(\lambda^2)$. Because λ^2 bears a small negative imaginary part, the pole moves just above the integration contour. At E it reverses its motion, and moves to $-\infty$ when s goes to 4. These results show that the transcendental (logarithmic or arctangent) factor of K stays on its principal sheet when $\frac{1}{2}(M^2-1)<\lambda^2<(M-1)^2$, and

$$\mathrm{Im}K(s,\lambda^2-i\epsilon)=\pi s/[U(s)]^{1/2},\quad s_-(\lambda^2)<s<s_+(\lambda^2),\quad \tfrac{1}{2}(M^2-1)<\lambda^2<(M-1)^2;$$
$$=0,\quad \text{other } s>4,\quad \tfrac{1}{2}(M^2-1)<\lambda^2<(M-1)^2. \quad (3.6)$$

Range 2: $M+1<\lambda^2<\frac{1}{2}(M^2-1)$

We condense our discussion. The same analysis as that given for range 1 applies to range 2 with one delicate modification: the point of reversal E in Fig. 3 disappears. As s decreases from $(M-1)^2$ to 4, the pole progresses steadily to the right, passing $x=+1$ when $s=s_-(\lambda^2)$. However, this alteration in no way affects the conclusions as to the branch of K. The transcendental factor of K remains on its principal sheet for all s and $M+1<\lambda^2<\frac{1}{2}(M^2-1)$. The imaginary part of K is still given by (3.6) for λ^2 in range 2.

Range 3: $4\leqslant\lambda^2<M+1$

The analysis given for range 1 applies to range 3 as long as $s>(M+1)^2$. However, now $R(s,\lambda^2)$ vanishes for some s in the range $(M-1)^2\leqslant s\leqslant(M+1)^2$. Thus the pole pushes through the integration contour in Fig. 3 when $s=s_0(\lambda^2)$, where

$$s_0(\lambda^2)=M^2+3-2\lambda^2. \tag{3.7}$$

In order to remain on the physical sheet of $K(s,\lambda^2-i\epsilon)$, we must deform the integration contour so that it remains ahead of the intruding pole. We adopt the equivalent procedure of allowing the pole to jump across the contour, picking up the discontinuity as an additive term. In this way K is analytic at s_0, but is now given by the expression

$$\begin{aligned}K(s,\lambda^2-i\epsilon)&=\frac{s}{[U(s)]^{1/2}}\int_{-1}^{1}\frac{dx}{x-R(s,\lambda^2-i)/[U(s)]^{1/2}},\\ &\qquad s>s_0(\lambda^2),\quad 4\leqslant\lambda^2<M+1;\\ &=\mp\frac{2\pi i}{[U(s)]^{1/2}}+\frac{s}{[U(s)]^{1/2}}\\ &\quad\times\int_{-1}^{1}\frac{dx}{x-R(s,\lambda^2-i\epsilon)/[U(s)]^{1/2}},\\ &\quad(M-1)^2<s<s_0(\lambda^2),\quad 4\leqslant\lambda^2<M+1.\end{aligned}\tag{3.8}$$

The (minus, plus) sign in (3.8) goes with the (upper, lower) branch of $[U(s)]^{1/2}$. We see that K remains independent of the branch of $[U(s)]^{1/2}$ taken between $(M-1)^2$ and $(M+1)^2$.

Now we encounter a branch point of $K(s,\lambda^2-i\epsilon)$ at $s=(M-1)^2$. This non-Landau singularity is related to that of the KT kernel at $s=(M+1)^2$ for $4\leqslant\lambda^2<M+1$, but now it is found at the lower branch point of $[U(s)]^{1/2}$. We should point out that one of these branch points of $[U(s)]^{1/2}$ is necessarily a singularity of K for $4\leqslant\lambda^2<M+1$. This is due to the fact that when R vanishes at s_0, the arctangent factor of K passes to its second sheet.

As yet, we have no instruction of how to pass the branch point of K at $s=(M-1)^2$. The instruction we need is given by Fig. 1. Just as we pass from range 3 to range 4, the branch point $s_+(\lambda^2)$ passes through $s=(M-1)^2$ into the lower half s plane. We cannot permit ourselves to cross the trajectory AB of $s_+(\lambda^2)$ without passing onto an unphysical sheet of K. The situation is analogous to the onset of an anomalous threshold for a loosely bound system. In that case a branch point of the spectral function crosses the integration contour as an internal mass like λ^2 is changed. The branch point pushes the contour ahead of it, and an anomalous threshold appears.[7] In our case the cut structure is not altered, since AB is within ϵ of the real s axis. Nevertheless, we must take care to stay on the physical sheet of K, and to do this we must choose the lower sign in (3.8). We note that for $(M-1)^2<s<s_0(\lambda^2)$, the arctangent factor of K is between $\pi/2$ and π. In (3.9) we will see that for $s_+(\lambda^2)<s<(M-1)^2$ the logarithm factor of K has the imaginary part $2\pi i$. Only in the region $s_+(\lambda^2)<s<s_0(\lambda^2)$, $4\leqslant\lambda^2<M+1$ is the transcendental factor of K off its principal sheet.

We have seen that we must pass below the non-Landau singularity at $s=(M-1)^2$, and also under the branch point $s_+(\lambda^2)$, even though the negative imaginary part attached to λ^2 would cause us to pass above $s_+(\lambda^2)$. When this is taken into account, we find that there is a deformation of the x-integration contour in Fig. 3 as we pass $s_-(\lambda^2)$. When this second deformation is taken into consideration, we find that

$$\begin{aligned}\mathrm{Im}K(s,\lambda^2-i\epsilon)&=2\pi s/[U(s)]^{1/2},\\ &\qquad s_+(\lambda^2)<s<(M-1)^2,\quad 4\leqslant\lambda^2<M+1;\\ &=\pi s/[U(s)]^{1/2},\\ &\qquad s_-(\lambda^2)<s<s_+(\lambda^2),\quad 4\leqslant\lambda^2<M+1;\\ &=0,\quad\text{other } s>4,\quad 4\leqslant\lambda^2<M+1.\end{aligned}\tag{3.9}$$

Now let us examine the implications of what we have found. From (3.6) and (3.9) we see that even in the physical decay region, $4\leqslant s\leqslant(M-1)^2$, perturbation theory disagrees with KT by the presence of the extra imaginary part $\mathrm{Im}K(s,\lambda^2-i\epsilon)=2\pi s/[U(s)]^{1/2}$ for $s_+(\lambda^2)<s<(M-1)^2$, and $4\leqslant\lambda^2<M+1$. This contradiction seems to imply that if we believe perturbation theory, then $M_0(s)$ as given by (2.5) is not the s-wave projection of M after all. We take the resolution of this apparent paradox to be the following. Suppose that in the KT representation M^2 has to be given a small positive imaginary part $+i\delta$ in order for the branch of $K(s,\lambda^2-i\epsilon)$ to be properly chosen. Our claim is that it is the $+i\delta$ attached to M^2 which specifies the physical branch of K, not the $-i\epsilon$ attached to λ^2. If this alternative boundary prescription is correct, then

$$K(s,\lambda^2)=\frac{s}{[U(s)]^{1/2}}\int_{-1}^{1}\frac{dx}{x-\dfrac{R(s,\lambda^2)}{[U(s)]^{1/2}}-i\delta\dfrac{\partial}{\partial M^2}\left\{\dfrac{R(s,\lambda^2)}{[U(s)]^{1/2}}\right\}}. \tag{3.10}$$

Using (3.10) one can show that $K(s,\lambda^2)$ is now consistent with perturbation theory.[8] Briefly, this is because $s_+(\lambda^2)$ never crosses into the lower half s plane in Fig. 1. At the same time the cut of $[U(s)]^{1/2}$ moves

[7] S. Mandelstam, Phys. Rev. Letters 4, 84 (1960).

[8] In Barton and Kacser[4] the possibility of second-type singularities on the physical sheet was overlooked. Thus their spectral function does not agree with the results of Sec. 3.

slightly into the upper half s plane. Thus one never need take s off the real s axis when considering (s,M^2) as complex variables. It was essentially the necessity of ducking under $s_+(\lambda^2)$ for $4\leqslant\lambda^2<M+1$ that led to the discrepancy between KT and perturbation theory when (s,λ^2) were taken as complex variables.

The branch of $K(s,\lambda^2)$ obtained using the boundary prescription $M^2\to M^2+i\delta$ has been discussed by Anisovich, Ansel'm, and Gribov.[9] However, as we have emphasized before, initially we are given the boundary prescription $\lambda^2\to\lambda^2-i\epsilon$ by KT, and an analysis such as that presented in this section is required to show the relevance of the work cited above.

4. GENERAL PERTURBATION THEORY RESULTS

In the previous section we have shown explicitly that analytic continuation of the spectral function for $f(s,M^2,\lambda^2)$ may be carried out with respect to M^2 or to λ^2. The results are unique in each case and agree, provided adequate care is taken when the continuation is made in λ^2. In this section we rederive the same results using the general methods developed for studying analyticity properties in perturbation theory.[10] We wish to see in a more general context what requires us to take special precautions when λ^2 is chosen as the second complex variable. In addition, we want to extend the usual analysis to include the determination of whether second-type singularities are present on the physical sheet. Our approach will not make use of the actual reason why second-type singularities exist. Rather we take the simpler view that since they are in evidence in the explicit spectral function, they must be included in a consideration of the singularities of the amplitude. Thus for the sake of clarity we deliberately restrict our methods.

We first consider the triangle graph of Fig. 2(b) as a function of the two complex variables s and M^2 for fixed real arbitrary $\lambda^2>4$. This is essentially the Barton and Kacser[4] analysis, but it includes the possibility of second-type singularities being present. We prove that the amplitude satisfies a Mandelstam representation in s and M^2, being analytic in the product of the two planes cut along the real axes $4\leqslant s<\infty$ and $(\lambda+1)^2\leqslant M^2<\infty$. This immediately enables us to perform analytic continuations in M^2 for both the amplitude and the spectral function, which lead to the same results as presented in Sec. 3. The conclusion is that $M^2+i\delta$ is a satisfactory perturbation theory prescription *even* in the presence of second-type singularities on the physical sheet.

To resolve the apparent conflict with the dispersion theory $\lambda^2-i\epsilon$ prescription, we finally consider s and λ^2 as complex variables, for fixed $M^2>9$. Such an *internal* variable analysis has not been carried out before, so we give full details. We find that there are complex singularities. These do not prevent analytic continuation in λ^2 of the single s-variable dispersion relation satisfied by the amplitude. However the complex singularities do prevent a straightforward λ^2 continuation of the spectral function. The prescription for dealing with this is easily obtained, and agrees precisely with that given in Sec. 3.

4.1 The (s,M^2) Analysis

We have

$$f(s,M^2,\lambda^2)=\int_0^1 d\alpha_1\int_0^1 d\alpha_2\int_0^1 d\alpha_3\,\delta\Big(\sum_i\alpha_i-1\Big)\Lambda^{-1} \tag{4.1}$$

$$\Lambda=\alpha_1\lambda^2+\alpha_2+\alpha_3-\alpha_1\alpha_2-\alpha_2\alpha_3 s-\alpha_3\alpha_1 M^2-i\epsilon \tag{4.2}$$

$$\Lambda=\alpha_i z_{ij}\alpha_j\equiv\alpha Z\alpha \tag{4.3}$$

with

$$z_{ij}=\begin{pmatrix}\lambda^2 & \frac{1}{2}\lambda^2 & \frac{1}{2}(\lambda^2+1-M^2)\\ \frac{1}{2}\lambda^2 & 1 & \frac{1}{2}(2-s)\\ \frac{1}{2}(\lambda^2+1-M^2) & \frac{1}{2}(2-s) & 1\end{pmatrix}$$

$$=y_{ij}(\lambda)^{\delta_{i1}+\delta_{j1}}\,, \tag{4.4}$$

where $y_{ij}=(m_i^2+m_j^2-p_{ij}^2)/2m_im_j$. By inspection, Λ never vanishes in the undistorted region of α integrations for the following domains (recall $y_{12}=\frac{1}{2}\lambda>1$):

(a) $\mathrm{Im}s>0$, $\mathrm{Im}M^2>0$;

(b) All $y_{ij}\geqslant 0$; i.e., $s\leqslant 2$, $M^2\leqslant 1+\lambda^2$;

(c) $|y_{23}|\leqslant 1$, $y_{13}\geqslant 0$;
i.e., $0\leqslant s\leqslant 4$, $M^2\leqslant 1+\lambda^2$;

(d) $|y_{13}|\leqslant 1$, $y_{23}\geqslant 0$;
i.e., $s\leqslant 2$, $(\lambda-1)^2\leqslant M^2\leqslant(\lambda+1)^2$. (4.5)

In (b)–(d) we consider only real variables.

The possible singularities of f are:

(1) *Normal thresholds.* $y_{13}=-1$ and $y_{23}=-1$. These are at $M^2=(\lambda+1)^2$ and $s=4$. From (b) above, the cuts are to be taken to $s=\infty$ and $M^2=\infty$.

(2) *The leading Landau curve* Γ. $\det y_{ij}=0$. This is

$$\Gamma\equiv s^2\lambda^2+s\lambda^4-s\lambda^2(M^2+3)+(M^2-1)^2=0. \tag{4.6}$$

(3) *The non-Landau singularity curve* Σ. This is the locus of (s,M^2) for which the three external momenta are collinear.[6] One finds immediately

$$\Sigma\equiv[s-(M-1)^2][s-(M+1)^2]$$
$$\equiv s^2-2s(M^2+1)+(M^2-1)^2=0. \tag{4.7}$$

Γ and Σ touch at two real points X and Y.

$$X\colon\ s=(\lambda^2-2)^2,\quad M^2=(\lambda^2-1)^2,\quad s=(M-1)^2$$
$$Y\colon\ s=0,\quad M^2=1. \tag{4.8}$$

[9] V. V. Anisovich, A. A. Ansel'm, and V. N. Gribov, Zh. Eksperim. i Teor. Fiz. **42**, 224 (1962) [translation: Soviet Phys.—JETP **15**, 159 (1962)].

[10] L. D. Landau, Nucl. Phys. **13**, 181 (1959).

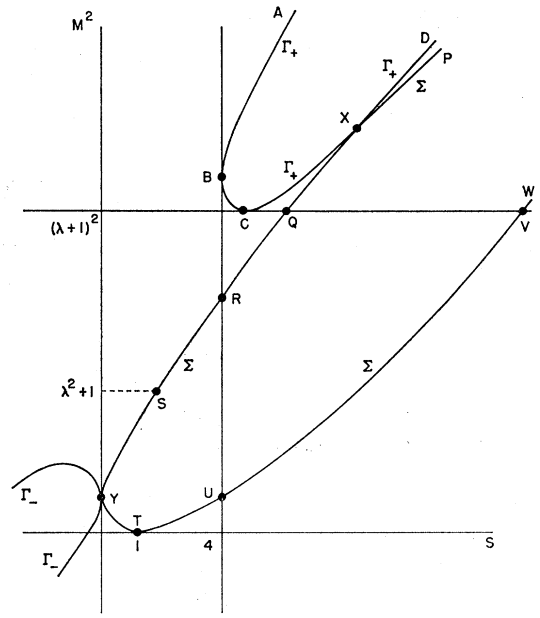

FIG. 4. The Landau and non-Landau surfaces in the real (s,M^2) plane. The various points are at: B, $M^2=2\lambda^2+1$; C, $s=M+1=\lambda+2$; X, $s=(\lambda^2-2)^2$, $M^2=(\lambda^2-1)^2$; R, $M^2=9$; Y, $M^2=1$; U, $M^2=1$.

This may be shown either by an extension of standard dual diagram analysis, or simply by looking at the simultaneous solutions of (4.5) and (4.6). We show the real section of the singularity curves in Fig. 4, in which the relative location of all points is correct. Γ_- and Γ_+ are the two branches of the hyperbola Γ; Σ is a parabola. From (4.5) we see that Γ_- is nonsingular on the physical sheet. Likewise, the $SYTU$ arc of Σ is nonsingular on the physical sheet. Since Σ and Γ have no real or complex common points other than X and Y, one may continue along the complex surface starting on Γ_- and reach Γ_+ without reaching any point where Γ can become singular. Thus there are no complex singularities associated with Γ, nor are the real arcs of Γ_+ singular in their curve limits. In the usual way the arcs $ABCX$ of Γ_+ can be made singular by continuing around the normal thresholds, thus arriving at the noncurve limits. At this point we cannot say anything about the arc DX in the noncurve limit. (So far we have just repeated the method of Barton and Kacser[4]; see also.[11])

We now turn to Σ. We have seen that the arc $SYTU$ of Σ is nonsingular, and hence neither are the complex Σ surfaces leaving $SYTU$, as long as they do not make contact with other singularities. This enables us to continue over the entire complex surface, and all of the real section, in the curve limits. Since $QRSYTUV$ lies below the M^2 cut, the distinction between curve and noncurve limits disappears, so that this part of the real section is never singular. We are left only QXP and VW as possible singularities of Σ in the noncurve limits.

[11] M. Fowler, P. V. Landshoff, and R. W. Lardner, Nuovo Cimento **17**, 956 (1960).

We do not examine the singularity of DX, QXP, and VW in the noncurve limits here, for to do so would involve us in a detailed consideration of the cause of second-type singularities not relevant to our present purpose. We have proved that f has no complex singularities for fixed $\lambda^2>4$. Thus

$$f(s,M^2,\lambda^2)=\frac{1}{\pi^2}\int_4^\infty \frac{ds'}{s'-s-i\epsilon} \times\int_{(\lambda+1)^2}^\infty \frac{dM'^2}{M'^2-M^2-i\epsilon}\beta(s',M'^2,\lambda^2) =\frac{1}{\pi}\int_4^\infty \frac{ds'}{s'-s-i\epsilon}\rho(s',M^2,\lambda^2). \tag{4.9}$$

Here β is the Bonnevay spectral function.[12]

Both the amplitude f and the spectral function ρ can be analytically continued in M^2, provided M^2 goes above the branch point at $(\lambda+1)^2$. The correct prescription is indeed obtained by putting $M^2\to M^2+i\delta$ in ρ, as already done at the end of Sec. 3.

4.2 The (s,λ^2) Analysis

We return to (4.1)–(4.4), but treat M^2 as real and fixed >9, taking s and λ^2 as the complex variables.

Λ never vanishes in the undistorted region of α integration for the domains

(a) $\mathrm{Im}s>0$, $\mathrm{Im}\lambda^2<0$.

(b) All $z_{ij}\geqslant 0$, i.e., $s\leqslant 2$, $\lambda^2\geqslant M^2-1$ (here s and λ^2 are real). (4.10)

The form $\Lambda=\alpha Z\alpha$ is a homogeneous quadratic form and hence it has end point and coincident singularities obtained by the usual criteria applied to the matrix Z. The possible singularities are:

(1) *Single contraction, single real coincidence.*

$$\begin{aligned}
&\alpha_1=0\colon\ s=4,\quad \alpha_2/\alpha_3>0\\
&\qquad\ s=0,\quad \alpha_2/\alpha_3<0\\
&\alpha_2=0\colon\ \lambda^2=(M-1)^2,\quad \alpha_1/\alpha_3>0\\
&\qquad\ \lambda^2=(M+1)^2,\quad \alpha_1/\alpha_3<0\\
&\alpha_3=0\colon\ \lambda^2=4,\quad \alpha_1/\alpha_2>0\\
&\qquad\ \lambda^2=0,\quad \alpha_1=1,\quad \alpha_2=0.
\end{aligned} \tag{4.11}$$

Thus the contractions give physical sheet singularities at $s=4$, at $\lambda^2=(M-1)^2$, and at $\lambda^2=0$.[13]

[12] G. Bonnevay, in *Proceedings of the 1960 Annual International Conference on High-Energy Physics at Rochester* (Interscience Publishers Inc., New York, 1960), p. 523.

[13] We emphasize that all the other singularities in (4.11) are not on the physical sheet, and that the contraction singularities found on the physical sheet are independent of each other. It is irrelevant when approaching the nonphysical singularity at $\lambda^2=4$ whether one has passed above or below the branch point at $\lambda^2=(M-1)^2$, since the latter branch point is not a feature of the comatrix of z_{33}. This is a novel feature of an analysis in terms of an internal mass.

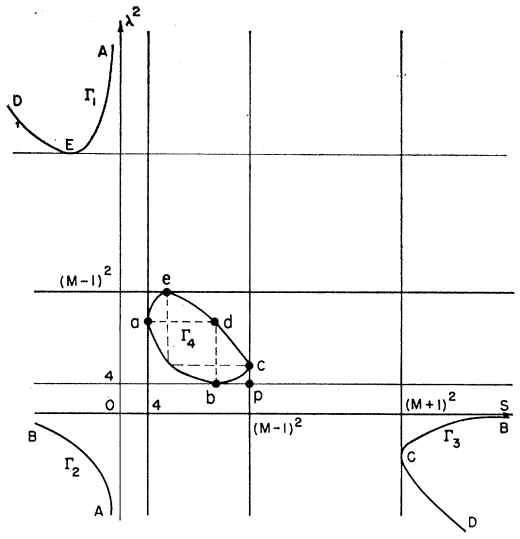

FIG. 5. The Landau surface in the real (s,λ^2) plane. The various points are at: a, $\lambda^2=\frac{1}{2}(M^2-1)$; b, $s=\frac{1}{2}(M^2-1)$; c, $\lambda^2=M+1$; e, $s=M+1$; C, $\lambda^2=-M+1$; E, $s=-M+1$.

(2) *The Landau singularity curve.* This is given by $\det z_{ij}=0$, which immediately reduces to $\det y_{ij}=0$. We obtain the singularity curve Γ as given in (4.6).

(3) *The non-Landau singularities (4.7).*

The real section of all possible singularity curves is shown in Fig. 5. Γ is tangent to the four lines $\lambda^2=0$, 4, $(M-1)^2$ and $(M+1)^2$, and because of its (s,λ^2) symmetry to the same lines with s replacing λ^2. We warn the reader that the (s,λ^2) symmetry does not hold as regards analyticity.

We can now use the techniques developed by Tarski[14] and Cook and Tarski[15] to analyze whether the possible curves are in fact singular on the physical sheet. In particular we use theorem 3.2 of Ref. 15 which states: If a singularity curve S is tangent to the one-further-contraction curve T, which is singular in a particular limit, then in that limit S is singular on one side of the point of tangency, and nonsingular on the other side. Conversely, if in some limit T is nonsingular, in that limit the two sides of S are either both singular or both nonsingular.[16]

With these preparations, we now identify the physical sheet singularities of f. We start on the real curve Γ_1 in Fig. 5, which from (4.10) is nonsingular. We can continue on the complex surfaces leaving Γ_1 and arrive at Γ_4 without becoming singular. Thus the arcs *ae* and *ed* of Γ_4 are nonsingular in the curve limits. We can move past d to arc *dc* on Γ_4, and from there along the complex surface to DC on Γ_3 without encountering a singularity on the physical sheet. However, by going around the appropriate singular normal thresholds we can reach the arcs *ae* and *edc* in their noncurve limits, in which they are singular.

We now concentrate on Γ_4. We know that *ae* is nonsingular in its curve limits (+,+) and (−,−), and singular in the other limits (+,−) and (−,+). Furthermore, the tangent at a, which is the one-further-contraction curve, is singular in all limits. Thus by the theorem quoted, the arc *ab* is singular in the (+,+) and (−,−) limits and nonsingular in the (+,−) and (−,+) limits. The latter are the appropriate curve limits, so the complex surfaces *abAB* are nonsingular.

From the arc *ab* of Γ_4, we continue our analysis to the arc *bc*. The tangent at b is the appropriate one-further-contraction curve, and it is nonsingular in all limits. Hence *bc* is singular in the limits (+,+) and (−,−) and nonsingular in the limits (+,−) and (−,+). The former limits, which are singular, are the curve limits, so the whole of the complex surfaces *bcBC* are singular.

This analysis has not relied on any detailed discussion of the non-Landau singularities, nor even the somewhat unusual singularity at $\lambda^2=0$. The complex singularities which we have found include, as a particular case, those in s for λ^2 real, $0<\lambda^2<4$, previously discussed in Refs. 11 and 17. Their presence prevents us from writing a double dispersion representation in s and λ^2. However, we can write a single variable representation in s for real $\lambda^2>(M-1)^2$.

$$f(s,M^2,\lambda^2)=\frac{1}{\pi}\int_4^\infty \frac{ds'}{s'-s-i\epsilon}\rho(s',M^2,\lambda^2), \qquad \lambda^2>(M-1)^2 \quad (4.12)$$

with

$$\rho(s,M^2,\lambda^2)=f(s+i\epsilon,M^2,\lambda^2)-f(s-i\epsilon,M^2,\lambda^2). \quad (4.13)$$

We now attempt to continue (4.12) and (4.13) analytically in λ^2 onto its physical cut; i.e., we go around the branch point $\lambda^2=(M-1)^2$ from below. For s in its upper half-plane, the continuation can be performed immediately (4.10a); thus the left-hand side of (3.12) can be analytically continued in λ^2. Further, for all real $\lambda^2>4$, there are no complex singularities in s, so the right-hand side of (4.12) still stands. Next we consider how the continuation of ρ can be carried out in (4.13). The term $f(s-i\epsilon,M^2,\lambda^2)$ causes some difficulty since for s in the range $(M-1)^2<s<(M+1)^2$ there are complex singularities in the lower half λ^2 plane. By following Fig. 5 in the (−,−) limit along the arc *BC*, then the complex surface with real s from C to c, and finally the arc *cb*, we can trace out the locus of the

[14] J. Tarski, J. Math. Phys. **1**, 149 (1960).
[15] L. F. Cook, Jr., and J. Tarski, J. Math. Phys. **3**, 1 (1962).
[16] The case in which both sides of S are singular and yet T is nonsingular seems paradoxial (see the remark at the end of Sec. 3 of Ref. 13), but is resolved when one realizes that the α_i integration contour may be pinched close to $\alpha_i=0$; yet due to some other branch cuts in the α_i plane, the contour detours around these other branch points before returning to $\alpha_i=0$. The only case that cannot occur is one where S is singular on one side of the point of tangency but not on the other, while T is nonsingular. For then one could drop a Cauchy integration loop over the singular arc of S, and so remove the singularity.

[17] P. V. Landshoff and S. B. Treiman, Nuovo Cimento **19**, 1249 (1961).

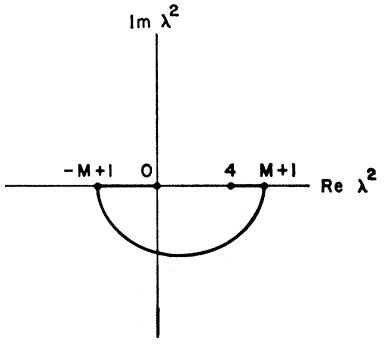

FIG. 6. The locus of one singularity of $\rho(s,M^2,\lambda^2)$ in the λ^2 complex plane.

singularity in the λ^2 plane. This locus is shown in Fig. 6. (Note that this singularity passes off the physical sheet at b in Fig. 5.) The locations of the points in Fig. 5 are $C:\lambda^2=-M+1$; $c:\lambda^2=M+1$; $b:s=\frac{1}{2}(M^2-1)$.

We see from Fig. 6 that we cannot immediately continue the spectral function $\rho(s,M^2,\lambda^2)$ into the region $4\leqslant\lambda^2<M+1$. This is precisely the special interval found in Sec. 3. However, the proper procedure at this point is immediately evident. We keep the negative imaginary term $-i\epsilon$ in $f(s-i\epsilon,M^2,\lambda^2)$ finite, continue in λ^2, and only as the last step let $\epsilon\to 0$. This corresponds to the "ducking" into the lower half-plane in Sec. 2, and keeps the singularities well down in the lower half λ^2 plane in Fig. 6 while the continuation is being carried out.

4.3 Further Comments on the Second-Type Singularities

Although we have not used any detailed properties of second-type singularities, we have not obtained complete information about them. In particular, in the (s,M^2) analysis we have not determined whether the second-type curves are singular on the physical sheet, in the noncurve limits, on the arcs PQR and VW of Fig. 4. The explicit continuations presented in Sec. 3 show that the arc XP is a physical sheet singularity of the spectral function ρ, and that this singularity lies in the upper half s plane. Accordingly, there is a second type singularity of the amplitude in the limit $s-i\epsilon$, $M^2+i\delta$ when $4\leqslant\lambda^2<M+1$.[18] In the (s,λ^2) analysis this corresponds to the portion cp of the singularity line $s=(M-1)^2$ in Fig. 5. No other parts of the non-Landau singularity curves are singular in any limit on the physical sheet for $\lambda^2>4$.

With these results we can present the Bonnevay spectral function $\beta(s,M^2,\lambda^2)$ introduced in (4.10), and correct the expression given by Barton and Kacser[4]. We have seen explicitly that ρ is real for $\lambda^2>(M-1)^2$, i.e., for M^2 below its threshold. Hence β is real and is therefore the imaginary part of ρ. β is nonzero only inside the region $ABCXP$ of Fig. 4, and from (3.8) and (3.11),

$$\beta(s,M^2,\lambda^2)=\pi\left[\frac{s(s-4)}{U(s)}\right]^{1/2} \text{ in } ABCXD \text{ of Fig. 4}$$

$$=2\pi\left[\frac{s(s-4)}{U(s)}\right]^{1/2} \text{ in } DXP \text{ of Fig. 4.} \qquad (4.14)$$

Barton and Kacser[4] failed to notice the support for β in region DXP. They also integrated over λ^2 from 4 to ∞. They found that the support for the Bonnevay spectral function for $F(s,M^2)$ is bounded by $s=4$ and arc RQP in Fig. 4. This conclusion is still correct.[19]

ACKNOWLEDGMENTS

It is a pleasure to acknowledge the useful discussions we had with M. Fowler, J. Tarski, and T. Truong. Our debt to Professor S. B. Treiman is very great, and this work owes its very existence to him.

[18] The argument against the existence of second-type singularities on the physical sheet given by Fairlie *et al.* Ref. 6 breaks down since the transcendental factor in ρ leaves its principal sheet. Barton and Kacser[4] also neglected this possibility.

[19] The conclusions expressed by (4.9) and (4.14) are equivalent to results obtained independently by C. Fronsdal and R. E. Norton, University of California, Los Angeles, preliminary report, March 1963 (unpublished). In particular, see their Fig. 4. They work only in the y_{ij} external variables, and so present only the equivalent of our (s,M^2) analysis. We are grateful to the authors for a copy of their report.